I&EC research
Industrial & Engineering Chemistry Research

Article

pubs.acs.org/IECR

# Studies on Mechanical Properties, Thermal Degradation, and Combustion Behaviors of Poly(1,4-butylene terephthalate)/Glass Fiber/Cerium Hypophosphite Composites

Wei Yang,[†,‡] Ningning Hong,[†] Lei Song,[†] Yuan Hu,*[,†] Richard K. K. Yuen,[‡] and Xinglong Gong*[,†,§]

[†]State Key Laboratory of Fire Science, University of Science and Technology of China and USTC-CityU Joint Advanced Research Centre, Suzhou, People's Republic of China

[‡]Department of Civil and Architectural Engineering, City University of Hong Kong and USTC-CityU Joint Advanced Research Centre, Suzhou, People's Republic of China

[§]CAS Key Laboratory of Mechanical Behavior and Design of Materials, Department of Modern Mechanics, University of Science and Technology of China

**ABSTRACT:** This work aims to develop glass-fiber reinforced poly(1,4-butylene terephthalate) (GRPBT) composites with enhanced mechanical, thermal stability, and flame retardancy properties using a novel compound, cerium hypophosphite (CHP). Mechanical performance studies showed that both the storage modulus and the tensile strength increased first and then decreased with increasing CHP content. For the GRPBT composite with 15 wt % of CHP, the storage modulus value at 30 °C was 3 times that of GRPBT. Thermogravimetric analysis (TGA) illustrated that low loading of CHP could improve the thermal stability of GRPBT composites. The volatilized esters measured by TGA coupled with FTIR (TGA-FTIR) in the decomposition of GRPBT with 20 wt % of CHP are decreased by about 69%. The combustion properties were evaluated by limiting oxygen index (LOI), Underwriters Laboratories 94 (UL 94), and cone calorimeter testing. For GRPBT containing 20 wt % of CHP, it achieved a V-0 classification with a high LOI (28.5%). Additionally, the peak heat release rate (PHRR) and total smoke production (TSP) were respectively reduced by around 76% and 45% as compared to the results obtained from GRPBT.

## 1. INTRODUCTION

Glass-fiber reinforced polymer matrix composites (GRPs) have become attractive engineering materials and are also one of the fastest growing plastics industry sectors because of their excellent mechanical properties, low density, low cost, and corrosion resistance. Conventional metallic materials are increasingly replaced by GRPs in many important sectors of industry such as aircraft, naval constructions, ships, buildings, and offshore structures.[1−3] However, most polymers are highly combustible due to their petroleum origin. The presence of glass fibers further enhances the flammability of polymer matrix due to their wick effect for the propagation of the combustion by increasing effectiveness of heat transmission in the burning area.[4] Consequently, the research and development of novel flame retarded GRPs is urgently needed to suppress their flammability.

Up to now, many types of flame retardant additives have been used to improve the flame retardancy in GRPs. Halogen- and organic phosphorus-based flame retardants have proved to be effective in inhibiting the combustion behavior of GRPs, but at the expense of negative environmental impacts and health concerns.[5,6] A number of nanoparticles (including clay, carbon nanotubes, carbon nanofibers, and polyhedral oligomeric silsesquioxanes) have also been studied to improve the flame retardancy of GRPs.[7−10] Although the incorporation of these nanoparticles can reduce the heat release rate in cone or microscale combustion calorimeter testing and enhance the mechanical performance of GRPs, the fire retardancy stays the same in the Underwriters Laboratories (UL) 94 testing. In our previous study, we found that the average flame time increased in UL 94 testing when a certain fraction of phosphorus-based flame retardant was substituted by nanoclay.[11]

Recently, aluminum diethyphosphinate has been found to be particularly effective to improve the flame retardancy of GRPs.[12−14] Braun and Schartel[12] fabricated a V-0 (UL 94 testing) glass-fiber reinforced poly(butylene terephthalate) (GRPBT) composite using aluminum diethyphosphinate and melamine cyanurate as a flame retardant mixture. They also studied the impact of different metal (Al, Zn) phosphinates on GRPBT composites.[13] The results showed that aluminum diethyphosphinate showed superior flame retardancy. Very recently, inorganic compound aluminum hypophosphite (AHP) was applied as a flame retardant in GRPs.[11,15,16] Even a low amount of AHP added can significantly enhance the fire retardancy of GRPs. Nevertheless, the thermal stability and mechanical properties of GRPs/AHP were seriously reduced. Thus, the application of AHP was greatly limited.

Inspired by the reported flame retardant effects provided by aluminum hypophosphite, another metal hypophosphite was taken into account to improve the fire retardancy performance of GRPs. In this study, trivalent cerium hypophosphite (CHP) was successfully synthesized. The aim of this work is to examine the use of CHP as a halogen-free flame retardant and

**Received:** January 19, 2012
**Revised:** June 3, 2012
**Accepted:** June 4, 2012
**Published:** June 4, 2012





dx.doi.org/10.1021/ie300176s | *Ind. Eng. Chem. Res.* 2012, 51, 8253−8261

reinforcement for glass-fiber reinforced poly(1,4-butylene terephthalate) (GRPBT) composites. The dynamic mechanical and tensile properties for these composites will be studied. The thermal decomposition process will be evaluated by TGA and TGA-FTIR. The combustion properties will be investigated by means of LOI, UL 94, and cone calorimeter.

## 2. EXPERIMENTAL SECTION

**2.1. Materials.** In this work, the studied composite is glass-fiber reinforced poly(1,4-butylene terephthalate) (PBT) composite. PBT (4500) was a product of BASF Chemical Co., Germany. Silane-coated short glass fiber (ECS-301CL, fiber diameter of 10 $\mu$m and initial fiber length of 3 mm) was supplied by Chongqing Polycomp International Co., Ltd., China. Trivalent cerium chloride heptahydrate (Sinopharm Chemical Reagent Co., Ltd.) was of analytical grade. Sodium hypophosphite (analytical reagent) was supplied by Tianjin Guangfu Fine Chemical Research Institute, China. Furthermore, the deionized water (ultrapure water) was used in this work.

**2.2. Synthesis of Cerium Hypophosphite.** In a typical experiment,[17] 2.00 g of sodium hypophosphite was dissolved in pH 1.4 (KCl−HCl) buffer solution (20 mL). The solvent used for the buffer solution was deionized water. 2.4 g of hydrated lanthanide chloride in the buffer solution (20 mL) was added. The reaction mixture was heated to 40 °C under reflux in a nitrogen atmosphere for 3 h. The resulting solids were collected by suction filtration, washed with water, and dried in the oven. Cerium hypophosphite (CHP) was synthesized via the typical method in this work. The rod-like crystals for CHP were formed, having sizes of about 4.0−20.0 $\mu$m in length and 0.9−4.8 $\mu$m in width. Characterized absorption bands from FTIR (KBr, $cm^{-1}$) are listed as follows: 2300−2450 ($PH_2$ stretching modes), 1100−1250 ($PH_2$ bending modes), 1079 (P−O modes), and 809 ($PH_2$ rocking modes).

**2.3. Preparation of GRPBT and GRPBT/CHP Composites.** PBT, CHP, and glass fiber were dried at 80 °C overnight before use. PBT was blended with additives using a twin-roll mill (XK-160, made in Jiangsu, China) at 235 °C for 10 min. The roller speed was 100 rpm for the preparation of all of the samples. They were then molded using a hot press at 235 °C under 5−10 MPa for 10 min to obtain 3.2 mm thick plaques. According to the reported data,[18] the mechanical properties of GRPBT are influenced by the flame retardant additives, but remain interesting for applications particularly because they can be optimized by adjusting the glass-fiber content to 25 or 30 wt %. Therefore, GRPBT and GRPBT/CHP composites with the same glass-fiber content of 30 wt % were investigated in the current work (Table 1).

**2.4. Measurements.** Dynamic mechanical analysis (DMA) was performed with the Perkin-Elmer Pyris Diamond DMA from 30 to 210 °C at a heating rate of 5 °C/min with a frequency of 10 Hz in the tensile configuration. The samples were cut from the compressed plaque, with dimensions 30 × 10 × 3.2 $mm^3$.

The tensile strength properties of GRPBT composites were investigated using a universal testing machine (WD-20D) according to the ASTM D-638 at room temperature. The specimens were prepared by cutting strips 4.0 ± 0.1 mm wide and 0.8 ± 0.3 mm thick. The crosshead speed was 20 mm/min. An average value of at least five individual determinations was obtained.

Thermogravimetric analysis (TGA) was carried out using a Q5000 IR thermogravimetric analyzer (TA Instruments Waters, China) at a linear heating rate of 20 °C/min in a nitrogen atmosphere. The weights of all of the samples were kept within 5−10 mg. Composites in an open Pt pan were tested under a gas-flow rate of 6 × $10^{-5}$ $m^3$ per minute at temperature ranging from room temperature to 700 °C.

Thermogravimetric analysis coupled with Fourier transform infrared spectroscopy (TGA-FTIR) of all composites had been performed using the TGA Q5000 IR thermogravimetric analyzer interfaced to the Nicolet 6700 FT-IR spectrophotometer. About 5.0 mg of each composite was put in an alumina crucible and heated from 30 to 700 °C. The heating rate was set as 20 °C/min in nitrogen atmosphere with a flow rate of 45 mL/min.

One group of combustion experiments was determined by limiting oxygen index (LOI) and Underwriters Laboratories (UL) 94 testing according to ASTM D2863 and the standard,[19] respectively. An HC-2 oxygen index meter (Jiangning Analysis Instrument Co., China) was used in the LOI testing. The specimens used for the test were of dimensions 100 × 6.5 × 3.2 $mm^3$. UL-94 testing was carried out on a CFZ-2-type instrument (Jiangning Analysis Instrument Co., China). The specimens used were of dimensions 130 × 13 × 3.2 $mm^3$.

The other combustion experiments were performed in a cone calorimeter (Fire Testing Technology) according to ASTM E 1354/ISO 5660. Each specimen (100 × 100 × 3.2 $mm^3$) was wrapped in an aluminum foil and exposed horizontally to 35 $kW/m^2$ external heat flux. Some residues collected in the cone calorimeter testing were further analyzed by means of the scanning electron microscope (SEM). The SEM micrographs were obtained with a scanning electron microscope AMRAY1000B at an accelerating voltage of 20 kV. The specimens were sputter-coated with a conductive layer.

**Table 1. Formulations and DMA Data for Each Sample**

| | composition (wt %) | | | storage modulus (GPa) | | |
|---|---|---|---|---|---|---|
| sample | PBT | glass fiber | CHP | 30 °C | 90 °C | 150 °C |
| GRPBT | 70 | 30 | 0 | 8.5 | 4.8 | 3.5 |
| GRPBT/CHP5 | 65 | 30 | 5 | 22.1 | 13.7 | 9.2 |
| GRPBT/CHP10 | 60 | 30 | 10 | 23.3 | 15.1 | 10.4 |
| GRPBT/CHP15 | 55 | 30 | 15 | 27.7 | 19.3 | 13.4 |
| GRPBT/CHP20 | 50 | 30 | 20 | 22.1 | 14.9 | 10.5 |

## 3. RESULTS AND DISCUSSION

**3.1. Dynamic Mechanical Properties.** Dynamic mechanical analysis (DMA) is one of the techniques commonly used to characterize the time, frequency, and temperature dependency of the viscoelastic nature of polymers.[20] As shown in Figure 1, the storage modulus of GRPBT is significantly improved with the introduction of rare earth hypophosphite. The trend in the variation of the storage modulus increases first and then decreases with increasing CHP concentration. The relevant data are summarized in Table 1. For instance, the GRPBT composite with 15 wt % of CHP exhibits a very high storage modulus value of about 27.7 GPa at 30 °C, which is 3 times that of GRPBT (about 8.5 GPa). The remarkable increase of storage modulus shows that the reinforcing effect dominates in the whole temperature region. Figure 1 also shows the variation of tan $\delta$ value in GRPBT composites with CHP concentration. The results show that the maximum of the tan $\delta$ curve shifts to higher temperature by the incorporation of CHP. The reason is


dx.doi.org/10.1021/ie300176s | Ind. Eng. Chem. Res. 2012, 51, 8253−8261

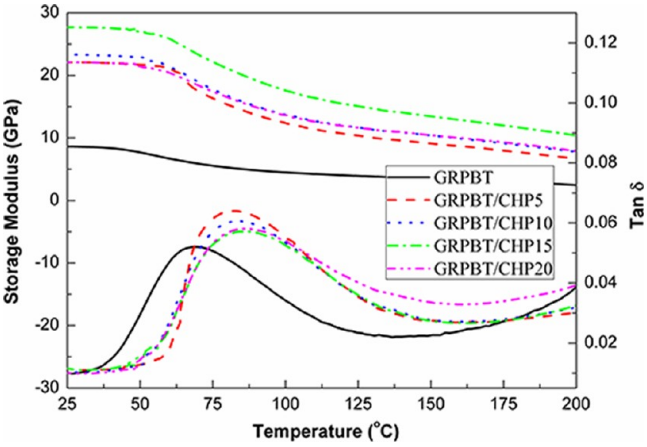


**Figure 1.** Storage modulus (top) and tangent delta (bottom) versus temperature from DMA measurements for GRPBT and GRPBT/CHP composites.

that the incorporation of the rod-like solid inorganic compound influences the movement of PBT chains, leading to the increased tan $\delta$ value.

**3.2. Tensile Properties.** Figure 2 shows the tensile properties of GRPBT and GRPBT/CHP composites with different CHP fraction. The tensile strength and elongation at break for GRPBT with 30 wt % of glass fibers are, respectively, 124 MPa and 2.73%. The results are consistent with the reported values.[18] From Figure 2a, it can be clearly observed that both the tensile strength and the tensile modulus increase first and then decrease with increasing CHP content. The tensile strength value increases from 124 MPa for GRPBT to 133 MPa for GRPBT/CHP10. Although the tensile strength and tensile modulus are reduced when the concentration of CHP is above 10 wt %, the two values for GRPBT composites with various CHP contents are larger than those for GRPBT. This means that the low loading of CHP to GRPBT leads to an enhancement of tensile properties. From Figure 2b, it is seen that the elongation at break decreases with increasing CHP content. Conceptually, inorganic/organic composites are often expected to become stiff and more brittle upon incorporation of inorganic fillers.[21] Because there is no reaction between the interface of PBT matrix and CHP, the compatibility is too poor to improve the elasticity of GRPBT composite, resulting in the reduction of strain-at-break. Additionally, the slightly decreased tensile strength and tensile modulus of GRPBT with high concentration of CHP are caused by the poor compatibility and aggregation of CHP particles in PBT matrix.

**3.3. Thermal Decomposition Analysis.** The mass and mass loss rate curves of CHP are shown in Figure 3. The

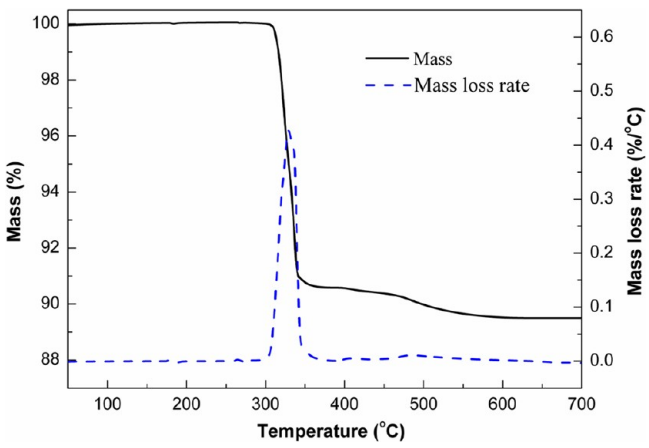


**Figure 3.** Mass and mass loss rate curves for CHP.

thermal decomposition of CHP begins from 323 °C ($T_{-3\%}$) with a maximum mass loss rate at 329 °C. Mass loss in the region of 323−350 °C results from the formation and release of phosphine due to the disproportionation of hypophosphite, occurring concomitantly with its partial oxidation.[17] The second thermal decomposition step after 350 °C is attributed to the release of $H_2O$. The thermal decomposition process of CHP could be represented by the two equations as detailed below:

$$2Ce(H_2PO_2)_3 \xrightarrow{\Delta} Ce_2(HPO_4)_3 + 3PH_3$$

$$2Ce_2(HPO_4)_3 \xrightarrow{\Delta} Ce_4(P_2O_7)_3 + 3H_2O$$

The resulting residue is of about 89.5 wt % and is mainly composed of cerium phosphates.

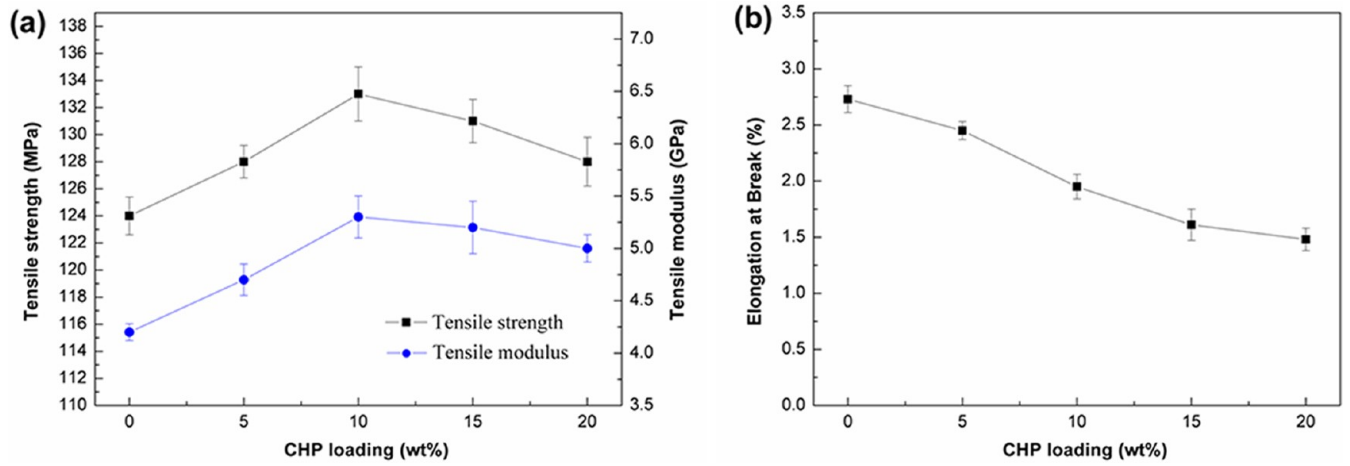


**Figure 2.** Tensile properties of GRPBT and GRPBT/CHP composites: (a) effect of CHP content on tensile strength and modulus; and (b) effect of CHP content on elongation at break.


dx.doi.org/10.1021/ie300176s | Ind. Eng. Chem. Res. 2012, 51, 8253−8261

The mass and mass loss rate curves of GRPBT and GRPBT/CHP composites are shown in Figure 4, and the results are

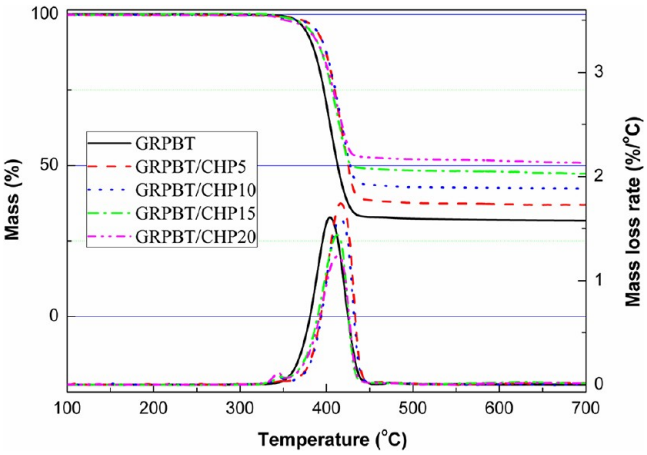


**Figure 4.** Mass (top) and mass loss rate (bottom) curves for GRPBT and GRPBT/CHP composites.

summarized in Table 1. The thermal decomposition of GRPBT in nitrogen atmosphere is characterized by a single decomposition step with maximum mass loss rate at 403 °C (Table 2). The resulting residue is of about 31.6 wt % and hence

**Table 2. TGA, DTG Data under Nitrogen Atmosphere for Each Sample**[a]

| sample | $T_{-3\%}$ (°C) | $T_{-30\%}$ (°C) | $T_{max}$ (°C) | residue (wt %) at 700 °C |
|---|---|---|---|---|
| GRPBT | 369 | 400 | 403 | 31.6 |
| GRPBT/CHP5 | 380 | 413 | 417 | 37.0 |
| GRPBT/CHP10 | 379 | 413 | 417 | 42.4 |
| GRPBT/CHP15 | 374 | 410 | 413 | 47.1 |
| GRPBT/CHP20 | 366 | 413 | 413 | 50.9 |

[a]20 °C/min, 5−15 mg; errors ±0.5 wt %, ±1 °C.

mainly composed of glass fibers. The decomposition of GRPBT is influenced by the addition of CHP. The decomposition temperature at 3 wt % mass loss ($T_{-3\%}$) is increased first and then decreased with increasing CHP content. Both the temperatures at 30 wt % mass loss ($T_{-30\%}$) and the maximum mass loss rate ($T_{max}$) for various GRPBT/CHP composites are higher than that of GRPBT. The results show that the incorporation of CHP improves the thermal stability of GRPBT. The residual weight is also improved by the addition of CHP. The high residual weight indicates that CHP probably reacts with PBT matrix. From the mass loss rate curves, it can be observed that the maximum mass loss rate of GRPBT is increased first and then reduced with the increasing fraction of CHP. This means that the pyrolysis of GRPBT is retarded by high loading of CHP. The weak peaks at around 345 °C for GRPBT/CHP composites should be attributed to the decomposition of CHP.

**3.4. Decomposed Product Analysis.** Identification of decomposition products was investigated by the TGA-FTIR technique, which could be used to distinguish the various inorganic and organic compounds from pyrolysis. The 3D infrared spectrum of evolved gases includes information of infrared absorbance, wavenumber, and temperature. From the 3D infrared spectrum, the change of spectral intensity along time direction corresponding to TGA results could be obtained. At the same time, when the wavenumber is fixed, absorbance information at different time is also obtained under the fixed wavenumber to analyze the certain component as a function of time. Because the linear relationship between time and temperature exists in the TGA-FTIR analysis, the current work illustrates the change of spectral intensity against temperature (Figure 5) and the absorbance information of various volatiles at different temperature (Figure 6) as detailed below.

The major gas products from the thermal decomposition of GRPBT include butadiene, carbon dioxide, tetrahydrofuran (THF), esters, and benzene derivatives. Main signals from the gas-phase spectra are assigned and summarized in Table 3. As shown in Figure 5a, a significant amount of esters (1727, 1267, and 1107 $cm^{-1}$) and butadiene (908 $cm^{-1}$) is released during the initial decomposition stage (384 °C) corresponding to $T_{-10\%}$ from TGA results. A few gases including THF (2965 and

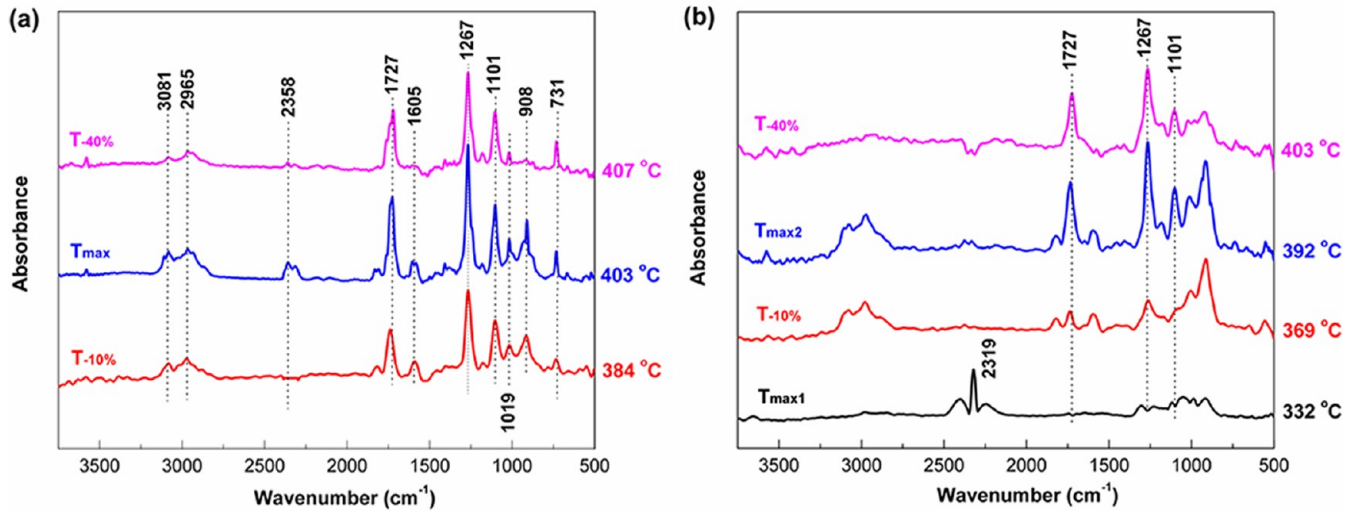


**Figure 5.** FTIR spectra of volatilized products at various temperatures during thermal decomposition of GRPBT (a) and GRPBT/CHP20 (b).


dx.doi.org/10.1021/ie300176s | Ind. Eng. Chem. Res. 2012, 51, 8253−8261

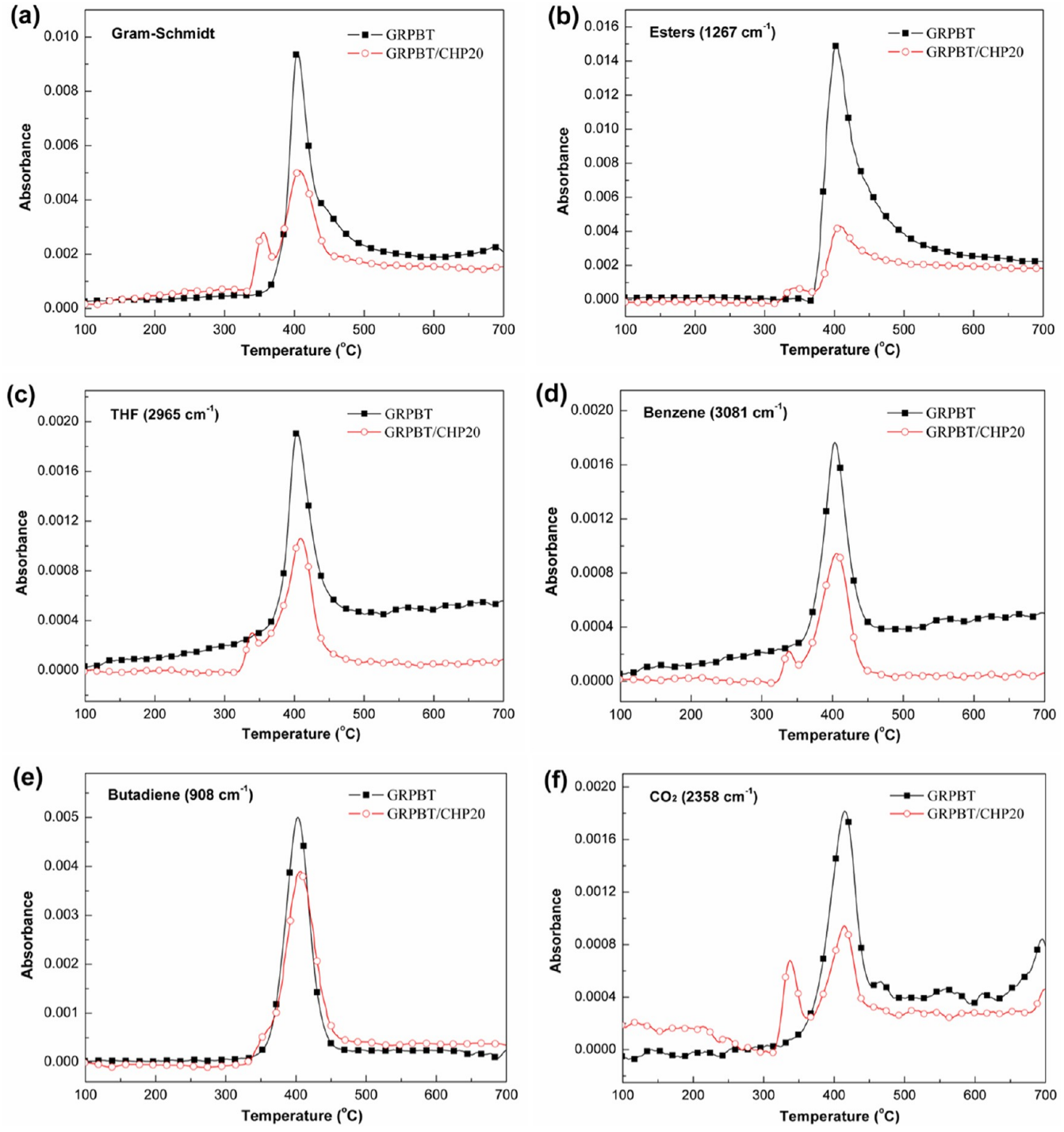


**Figure 6.** Absorbance of pyrolysis products for GRPBT and GRPBT/CHP20 composites versus temperature: (a) Gram−Schmidt; (b) esters; (c) THF; (d) benzene; (e) butadiene; and (f) $CO_2$.

**Table 3. Characteristic Attribution of FTIR Absorption Bands**

| band position ($cm^{-1}$) | assignment |
|---|---|
| 3081, 1605, 731 | benzene |
| 2965, 1019 | tetrahydrofuran (THF) |
| 2358, 668 | carbon dioxide ($CO_2$) |
| 1727, 1267, 1101 | esters |
| 908 | butadiene |
| 2319, 990 | $PH_3$ |

1019 $cm^{-1}$) and benzene (3081, 1605, and 731 $cm^{-1}$) are detected. Around the temperature at maximum mass loss rate (403 °C), the signals of various volatiles all become strong. Volatilization of esters is also obviously observed at the latter decomposition stages (425 and 445 °C). The thermal degradation process of GRPBT/CHP20 is shown in Figure 5b. Phosphine ($PH_3$, 2319 and 990 $cm^{-1}$)[22] is detected at 332 °C, which is the main product during the decomposition of CHP. At 369 °C ($T_{-10\%}$), the release of esters is significantly retarded as compared to GRPBT. This result shows that CHP probably reacts with PBT matrix leading to the reduction of


dx.doi.org/10.1021/ie300176s | Ind. Eng. Chem. Res. 2012, 51, 8253−8261

escaped esters. The last two FTIR spectra of GRPBT/CHP are similar to those of GRPBT. It is indicated that adding CHP into GRPBT does not fundamentally change the evolved products in the gas phase, but influences the product release rate.

To further understand the relationship between flame retardant additives and the gas-phase product release rate, the absorbance of pyrolysis products for GRPBT and GRPBT/CHP20 versus temperature is revealed. Figure 6a illustrates the absorbance intensity of the total gases (Gram−Schmidt) for the two composites. The other five figures respectively show the absorbance intensity of esters, THF, benzene, butadiene, and $CO_2$. Evidently, the evolved esters are significantly reduced by the incorporation of CHP. The result shows that CHP or the condensed-phase products of CHP probably react with PBT matrix or its products, resulting in the reduction of volatilized esters. In addition, the other pyrolysis products are all lower than those of GRPBT. It has been known that the incorporation of CHP into GRPBT promotes the formation of char residues. Some volatilized products are trapped in the degradation process, which participate in the charring reaction. The char layer becomes a barrier to the gas products, leading to the reduction of the total gases.

**3.5. Fire Retardancy Testing.** LOI and UL 94 tests were performed to determine the flame class of GRPBT and GRPBT/CHP composites. The results obtained from the two tests are summarized in Table 4. GRPBT is a flammable polymeric composite with a LOI of 22%. With increasing CHP concentration, the LOI increases. For the GRPBT composite that contains 20 wt % of CHP, the LOI value increases to 28.5%. GRPBT fails in UL 94 testing with a very long burning time. No melt flow or dripping is observed. It is probably the reason that the addition of glass fibers to PBT results in wick and antidripping effects.[4] The GRPBT composites containing low concentration of CHP also fail in UL 94 testing. When the fraction of CHP is 15 wt %, it could extinguish after the first application of the flame. The GRPBT composite containing 20 wt % of CHP achieves a V-0 rating, indicating the high flame retardant efficiency of CHP. In combination with thermal decomposition analysis, it has been known that the addition of CHP could promote the formation of condensed residues and reduce the release of volatilization products. Condensed residues covered on the surface of glass fibers may be effective to reduce the wick effect to enhance the self-extinguishment of GRPBT composites.

**Table 4. Results of UL-94 and LOI Testing for Each Sample**

| | | UL 94, 3.2 mm bar | | |
|---|---|---|---|---|
| sample | LOI (%) | $t_1/t_2$[a] (s) | dripping | rating |
| GRPBT | 22 ± 0.5 | BC[b] | yes | NR[c] |
| GRPBT/CHP5 | 26 ± 0.5 | BC | yes | NR |
| GRPBT/CHP10 | 27 ± 0.5 | BC | yes | NR |
| GRPBT/CHP15 | 27.5 ± 0.5 | 14.9/BC | yes | NR |
| GRPBT/CHP20 | 28.5 ± 0.5 | 1.0/6.9 | no | V-0 |

[a] $t_1$ and $t_2$, average combustion times after the first and the second applications of the flame. [b] BC, burns to clamp. [c] NR, not rated.

**3.6. Cone Calorimeter Testing.** Cone calorimeter is one of the most effective bench-scale methods for the laboratory evaluation of the fire performance of polymeric materials. The main parameters obtained from a cone calorimeter are commonly divided into three parts. The first part is heat release parameters including heat release rate (HRR) and total heat release (THR); the second is smoke emission data containing smoke production rate (SPR), total smoke production (TSP), and average specific extinction area (ASEA); the last is fire decomposition parameters including average mass loss rate (AMLR).[23,24] The cone calorimeter data obtained at a heat flux of 35 kW/m$^2$ for the GRPBT and GRPBT/CHP composites are summarized in Table 5. The HRR, THR, SPR, and TSP curves are shown in Figure 7. In each set of formulation, an increase in loading of CHP from 5% to 20% significantly reduces the PHRR and THR values. For example, the PHRR value decreases from 417 kW/m$^2$ for GRPBT to 101 kW/m$^2$ for GRPBT/CHP20 with a reduction of 76%. The THR value for GRPBT/CHP20 is reduced by around 20%. The results show that the fire hazards of GRPBT are remarkably reduced by the addition of CHP.

Figure 7c and d respectively shows the SPR and TSP curves for GRPBT and GRPBT/CHP composites. Both the peak of smoke production rate (PSPR) and the TSP increase first and then decrease, indicating that the production of smoke is high in low concentration of CHP. The trend in the variation of ASEA is similar to that of PSPR and TSP. All three values are significantly reduced by the addition of CHP with high concentration. For instance, the TSP value decreases from 352 m$^2$/kg for GRPBT to 195 m$^2$/kg for GRPBT/CHP20 with a reduction of about 45%. Similarly, the ASEA value for GRPBT/CHP20 is reduced by around 33%. The results also show that the incorporation of CHP could reduce the fire risks of GRPBT composites.

The reduction of fire hazards should be mainly attributed to the remarkable decrease of the mass loss rate. From the AMLR results, it can be seen that the AMLR value of GRPBT/CHP20 is reduced by around 69% in comparison with that of GRPBT. The reduction of mass loss rate may have resulted from the formation of char layer. The improved flame retardancy can also be reflected through the combustion efficiency, represented by the carbon monoxide/carbon dioxide ratio from the

**Table 5. Cone Calorimeter Data for Each Sample at 35 kW/m$^2$[a]**

| sample | TTI (s) | PHRR (kW/m$^2$) | THR (MJ/m$^2$) | AMLR (g/s/m$^2$) | ASEA (m$^2$/kg) | TSP (m$^2$/kg) | ACOY (kg/kg) | $ACO_2Y$ (kg/kg) | $R$ | CY (%) |
|---|---|---|---|---|---|---|---|---|---|---|
| GRPBT | 49 | 417 | 53.6 | 6.2 | 520 | 352 | 0.052 | 1.64 | 0.032 | 31.5 |
| GRPBT/CHP5 | 46 | 289 | 48.8 | 2.9 | 806 | 498 | 0.074 | 1.47 | 0.050 | 37.5 |
| GRPBT/CHP10 | 53 | 207 | 48.4 | 2.6 | 277 | 296 | 0.084 | 1.46 | 0.058 | 41.5 |
| GRPBT/CHP15 | 48 | 142 | 48.3 | 2.2 | 478 | 260 | 0.108 | 1.54 | 0.070 | 48.7 |
| GRPBT/CHP20 | 38 | 101 | 42.8 | 1.9 | 349 | 195 | 0.122 | 1.42 | 0.086 | 53.2 |

[a] TTI: time to ignition, ±2 s. PHRR: peak heat release rate, ±15 kW/m$^2$. THR: total heat release, ±0.5 MJ/m$^2$. AMLR: average mass loss rate, ±0.1 g/s/m$^2$. ASEA: average specific extinction area, ±20 m$^2$/kg. TSP: total smoke production, ±10 m$^2$/kg. ACOY: average CO yield, ±0.005 kg/kg. $ACO_2Y$: average $CO_2$ yield, ±0.008 kg/kg. $R$ = ACOY/$ACO_2Y$. CY: char yield, ±0.5%.


dx.doi.org/10.1021/ie300176s | Ind. Eng. Chem. Res. 2012, 51, 8253−8261

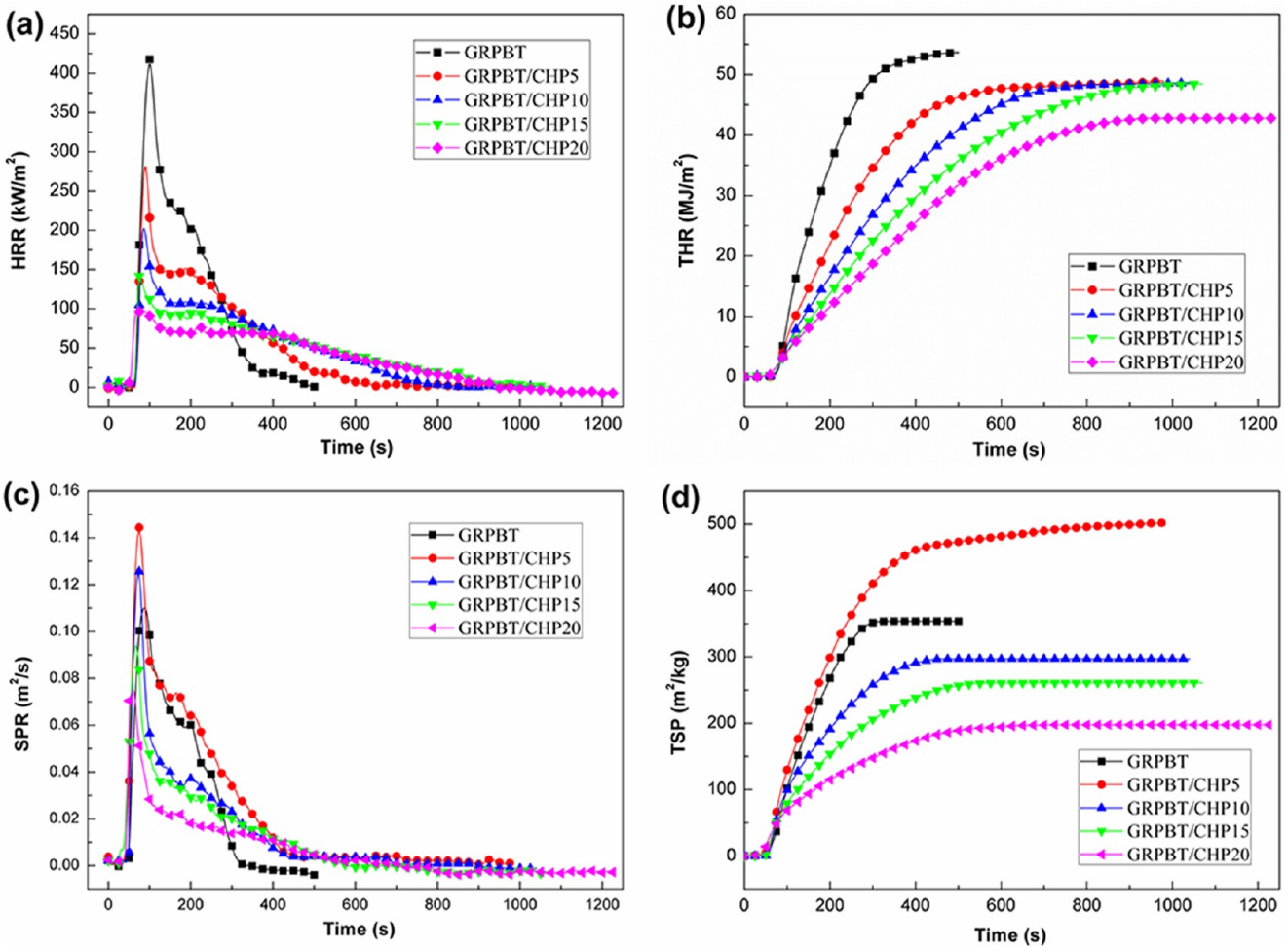


**Figure 7.** HRR (a), THR (b), SPR (c), and TSP (d) curves from cone calorimeter testing for GRPBT and GRPBT/CHP composites.

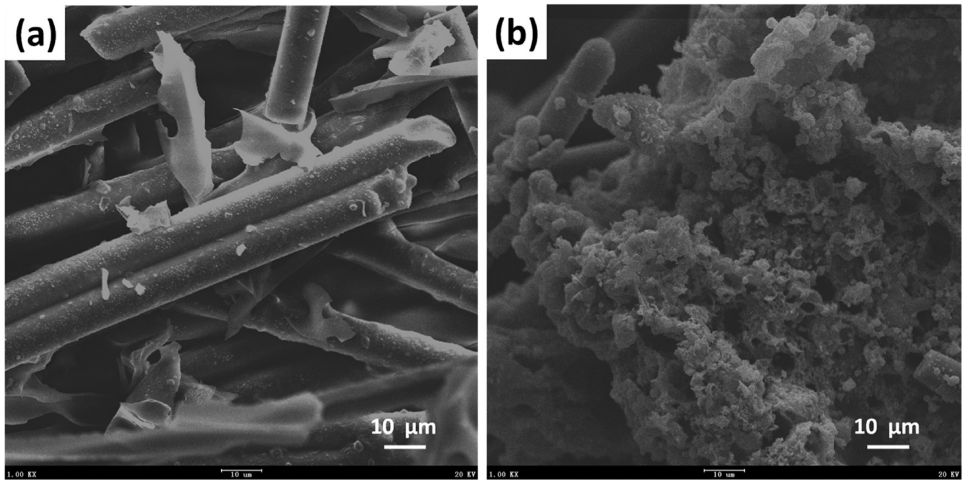


**Figure 8.** SEM images for the residues after cone calorimeter testing: (a) GRPBT; and (b) GRPBT/CHP20.

cone calorimeter data. In this work, the *R* value means the average CO yield/average $CO_2$ yield ratio. The *R* value increases with the increasing CHP content, indicating that the combustion of GRPBT/CHP composites is more incomplete than that of GRPBT. The results are consistent with PHRR and THR values. The evidence also demonstrates that the combustion of GRPBT is greatly inhibited by the introduction of CHP.

To realize the flame retardancy mechanism of GRPBT composites in the current work, the residues of GRPBT and GRPBT/CHP20 after cone calorimeter testing were analyzed by SEM (Figure 8). From Figure 8b, it is clearly observed that there is a mass of char residues around the glass fibers. From the TGA and cone calorimeter results, it has been known that residual weight of GRPBT is improved by the addition of CHP. Condensed char layer can reduce the mass loss rate of the


dx.doi.org/10.1021/ie300176s | *Ind. Eng. Chem. Res.* 2012, 51, 8253−8261

polymer matrix, leading to the reduction of combustible gases' concentration in the flame area. Moreover, the char layer can effectively decrease the heat conduction of glass fibers and cut off the mass transfer path, resulting in the weakening of the wick effect. Therefore, the flame retardancy is enhanced.

## 4. CONCLUSIONS

Halogen-free fire retarded GRPBT composites were prepared using cerium hypophosphite (CHP) as flame retardant filler. Micrometer-sized CHP was successfully synthesized. Mechanical performance studies showed that both the storage modulus and the tensile strength increased first and then decreased with increasing CHP content. Thermogravimetric analysis illustrated that low loading of CHP could improve the thermal stability of GRPBT composites. TGA-FTIR analysis showed that all of the volatilized products were reduced by the addition of CHP. The combustion properties were evaluated by limiting oxygen index (LOI), Underwriters Laboratories 94 (UL 94), and cone calorimeter testing. For the composite containing 20 wt % of CHP (GRPBT/CHP20), it achieved a V-0 classification with a high LOI (28.5%). Additionally, the peak heat release rate (PHRR) and total smoke production (TSP) values were respectively reduced by around 76% and 45% as compared to the results obtained from GRPBT. The improvement of flame retardancy was mainly caused by the condensed phase effect during the interaction of PBT matrix and CHP. In summary, low concentration of CHP can be well dispersed in PBT matrix, resulting in the enhancement of mechanical properties. Meanwhile, the thermal decomposition of PBT is inhibited by the barrier effect caused by the well dispersion. When the concentration of CHP is high, the dispersion becomes poor leading to the reduction of mechanical properties. Because the thermal decomposition temperature of CHP is lower than that of PBT, a large amount of volatiles is released earlier, resulting in the reduced thermal stability, when GRPBT contains a high concentration of CHP. CHP is also a good flame retardant for GRPBT. However, high concentration is needed to fulfill GRPBT high flame retardancy classification, such as self-extinguishing in a short time and no dripping.

## AUTHOR INFORMATION


### Corresponding Author

*(Y.H.) Tel./fax: +86-551-3601664. E-mail: yuanhu@ustc.edu.cn. (X.G.) Tel: +86-551-3600419. E-mail: gongxl@ustc.edu.cn.


### Notes

The authors declare no competing financial interest.

## ACKNOWLEDGMENTS

This work was financially supported by the National Natural Science Foundation of China (No. 50903080) and Program for Education combined with the production and research of Guangdong province and the Education Department of the Chinese government (No. 2009A090100010) and National Natural Science Foundation of China (No. 11125210).

## REFERENCES


(1) Mouhmid, B.; Imad, A.; Benseddiq, N.; Lecompte, D. An experimental analysis of fracture mechanisms of short glass fiber reinforced polyamide 6,6 (SGFR-PA66). *Compos. Sci. Technol.* **2009**, *69*, 2521−2526.

(2) Toldy, A.; Szolnoki, B.; Marosi, G. Flame retardancy of fiber-reinforced epoxy resin composites for aerospace applications. *Polym. Degrad. Stab.* **2011**, *96*, 371−376.

(3) Tang, Y.; Zhuge, J. F.; Lawrence, J.; Mckee, J.; Gou, J. H.; Ibeh, C.; Hu, Y. Flame retardancy of carbon nanofiber/intumescent hybrid paper based fiber reinforced polymer composites. *Polym. Degrad. Stab.* **2011**, *96*, 760−770.

(4) Casu, A.; Camino, G.; Giorgi, M. D.; Flath, D.; Laudi, A.; Morone, V. Effect of glass fibers and fire retardant on the combustion behaviour of glass fibers-poly(butylene terephthalate) composites. *Fire Mater.* **1998**, *22*, 7−14.

(5) Levchik, S. V.; Weil, E. D. Flame retardancy of thermoplastic polyesters-a review of the recent literature. *Polym. Int.* **2005**, *54*, 11−35.

(6) Zhao, Q.; Zhang, B. Q.; Quan, H.; Yam, R. C. M.; Yuen, R. K. K.; Li, R. K. Y. Flame retardancy of rice husk-filled high-density polyethylene ecocomposites. *Compos. Sci. Technol.* **2009**, *69*, 2675−2681.

(7) Isitman, N. A.; Gunduz, H. O.; Kaynak, C. Nanoclay synergy in flame retarded/glass fiber reinforced polyamide 6. *Polym. Degrad. Stab.* **2009**, *9*, 2241−2250.

(8) Shen, Z. Q.; Bateman, S.; Wu, D. Y.; McMahon, P.; Dell'Olio, M.; Gotama, J. The effects of carbon nanotubes on mechanical and thermal properties of woven glass fiber reinforced polyamide 6 nanocomposites. *Compos. Sci. Technol.* **2009**, *69*, 239−244.

(9) Zhao, Z. F.; Gou, J. H.; Bietto, S.; Ibeh, C.; Hui, D. Fire retardancy of clay/carbon nanofiber hybrid sheet in fiber reinforced polymer composites. *Compos. Sci. Technol.* **2009**, *69*, 2081−2087.

(10) Wu, K.; Kandola, B. K.; Kandare, E.; Hu, Y. Flame retardant effect of polyhedral oligomeric silsesquioxane and triglycidyl isocyanurate on glass fiber-reinforced epoxy composites. *Polym. Compos.* **2011**, *32*, 378−389.

(11) Yang, W.; Hu, Y.; Tai, Q. L.; Lu, H. D.; Song, L.; Yuen, R. K. K. Fire and mechanical performance of nanoclay reinforced glass-fiber/PBT composites containing aluminum hypophosphite particles. *Composites, Part A* **2011**, *42*, 794−800.

(12) Braun, U.; Schartel, B. Flame retardancy mechanisms of aluminium phosphinate in combination with melamine cyanurate in glass-fiber-reinforced poly(1,4-butylene terephthalate). *Macromol. Mater. Eng.* **2008**, *293*, 206−217.

(13) Braun, U.; Bahr, H.; Sturm, H.; Schartel, B. Flame retardancy mechanisms of metal phosphinates and metal phosphinates in combination with melamine cyanurate in glass-fiber reinforced poly(1,4-butylene terephthalate): the influence of metal cation. *Polym. Adv. Technol.* **2008**, *19*, 680−692.

(14) Braun, U.; Schartel, B.; Fichera, M. A.; Jager, C. Flame retardancy mechanisms of aluminium phosphinate in combination with melamine polyphosphate and zinc borate in glass-fiber reinforced polyamide 6,6. *Polym. Degrad. Stab.* **2007**, *92*, 1528−1545.

(15) Zhao, B.; Hu, Z.; Chen, L.; Liu, Y.; Liu, Y.; Wang, Y. Z. A phosphorus-containing inorganic compound as an effective flame retardant for glass-fiber-reinforced polyamide 6. *J. Appl. Polym. Sci.* **2011**, *119*, 2379−2385.

(16) Yang, W.; Song, L.; Hu, Y.; Lu, H. D.; Yuen, R. K. K. Enhancement of fire retardancy performance of glass-fiber reinforced poly(ethylene terephthalate) composites with the incorporation of aluminum hypophosphite and melamine cyanurate. *Composites, Part B* **2011**, *42*, 1057−1065.

(17) Seddon, J. A.; Jackson, A. R. W.; Kresiński, R. A.; Platt, A. W. G. Complexes of the lanthanide metals (La-Nd, Sm-Lu) with hypophosphite and phosphite ligands: crystal structures of $[Ce(H_2PO_2)_3(H_2O)]$, $[Dy(H_2PO_2)_3]$ and $[Pr(H_2PO_2)(HPO_3)(H_2O)]\cdot H_2O$. *J. Chem. Soc., Dalton Trans.* **1999**, *13*, 2189−2196.

(18) R&D Flame Retardants, Pigment & Additives Division, Clariant GmbH, public information presented at the 9. SKZ Fachtagung Kunststoffe, Brandschutz und Flammschutzmittel, Würzburg, December 5,6, 2007.

(19) UL 94: flammability of plastic materials for parts in devices and appliances, 2009.

(20) Quan, H.; Zhang, B. Q.; Zhao, Q.; Yuen, R. K. K.; Li, R. K. Y. Facile preparation and thermal degradation studies of graphite

nanoplatelets (GNPs) filled thermoplastic polyurethane (TPU) nanocomposites. *Composites, Part A* **2009**, *40*, 1506−1513.
(21) Tseng, C. H.; Hsueh, H. B.; Chen, C. Y. Effect of reactive layered double hydroxides on the thermal and mechanical properties of LDHs/epoxy nanocomposites. *Compos. Sci. Technol.* **2007**, *67*, 2350−2362.
(22) Bornemann, H.; Sander, W. Reactions of methyl(phenyl)-silylene with CO and $PH_3$-the formation of acid-base complexes. *J. Organomet. Chem.* **2002**, *641*, 156−164.
(23) Scudamore, M. J.; Briggs, P. J.; Prager, F. H. Cone calorimetry-a review of tests carried out on plastics for the association of plastic manufacturers in Europe. *Fire Mater.* **1991**, *15*, 65−84.
(24) Li, B. Influence of polymer additives on thermal decomposition and smoke emission of poly(vinyl chloride). *Polym. Degrad. Stab.* **2003**, *82*, 467−476.